Journal of Applied Polymer Science

Scatheless active functionalized poly(*p*-phenylene terephthalamide) fibres and their outstanding potential in enhancing interface adhesion with polymer matrix

Ye Yuan, Shaokun Song, Sufen Deng, Qin Wang, Qisong Feng, Chuanxi Xiong, Lijie Dong
School of Materials Science and Engineering, Wuhan University of Technology, Luoshi Road 122, Wuhan 430070, People's Republic of China
Correspondence to: L. Dong (E-mail: dong@whut.edu.cn)

ABSTRACT: Exploration of new functionalization approaches to inert rigid fiber, activation inert surface, and enhancing interface adhesion is urgently required for fiber-based multiphase materials. In this paper, we developed a simple yet efficient method towards active functionalized poly(*p*-phenylene terephthalamide) fiber through mussel-adhesive, self-polymerization, and successive dipping–drying procedure based on as-designed detachable equipment. In comparison with current acid etching and high energy radiation methods, the active functional strategy achieves scatheless functional modification to inert rigid fiber. Attribute to π–π conjugation effect, the new active nanolayers integrate rigid fiber and polymer matrix into homogeneous-like structure. Consequently, the functionalized fiber-based composites exhibit great mechanical property and desirable field-responsive ability. © 2015 Wiley Periodicals, Inc. J. Appl. Polym. Sci. **2016**, *133*, 43018.

KEYWORDS: compatibilization; fibers; functionalization of polymers; nanostructured polymers; structure–property relations

Received 19 May 2015; accepted 7 October 2015
DOI: 10.1002/app.43018

INTRODUCTION

Poly(*p*-phenylene terephthalamide) (PPTA) fiber is an aramid fiber with high modulus and high tensile strength. It has become quite popular for a variety of applications ranging from military part to daily life, for it is quite a reinforcing fiber in composite materials.[1,2] For fiber-reinforced polymer composites, it is well known that the mechanical property and functionality mainly depends on the interfacial adhesion between the fiber and the polymer matrix. Although PPTA has much more striking advantage, it exhibits low compatibility with thermoplastic materials, resin matrices and general elastomer owing to its chemically inert and very smooth surface.[3] Nowadays, the key challenge of PPTA-based composites in practical application is to activate the nonvalent surface for effectively enhancing the interface adhesion with target matrix by chemical or physical reaction without damaging its outstanding mechanical properties. However, current technology surrounding PPTA modification primarily focuses on acid etching,[4–8] high energy radiation,[9,10] ultrasound treatment,[11] or plasma treatment.[12–15] These methods roughen PPTAs smooth surface to enhance the interface adhesion. Obviously, the desirable mechanical performance of PPTA would be inevitably ruined because the surface of PPTA was damaged by acid-etch or strong radiation. Besides, these methods also involved complicated equipment, high energy consumption and serious environmental pollution issues.

In this paper, we developed a simple yet efficient method towards actively functionalize PPTA through mussel-adhesive, self-polymerization and successive dipping–drying procedure without any damaging for PPTA surface state. Successive dipping–drying processing was carried out on an assembly line with some detachable parts recently developed in our laboratory. The mussel-adhesive and self-polymerization are based on the conversion mechanism of dopamine (DOPA) into polydopamine (PDOPA) followed by the alkaline pH-induced oxidation of PDOPA.[16–20] The pristine fibril was dragged by rollers and impregnated into formulated DOPA solution through dipping vessels; In quick succession, warm oxygen was used to induce the self-polymerization of DOPA which was puffed on the surface of fiber by oxygen pipe between each dipping vessel. Regulating the dipping–drying cycles or time interval, the fibrils were coated with a sheath shell whose thickness could be controlled in nanometer scale. More importantly, PDOPA is also active layer for polymer matrix due to amino and hydroxyl

Additional Supporting Information may be found in the online version of this article.

groups rich in the layer. Hence this method which is carried out on the assembly line for functionalizing PPTA was economical and efficient, and also could be used in factory production. For exploring the interfacial adhesion potential, ethylene-propylene-diene-terpolymer grafted maleic anhydride (EPDM-*g*-MAH) was employed as the matrix to evaluate the surface treatments of PPTA and demonstrate the interfacial improvement mechanism between rubber matrices and active layers on PPTA. It also opens a path to integrated firmly active PPTA fiber into matrix, which will lead PPTA-based composite to expand more application fields.

EXPERIMENTAL

Materials

PPTA fiber was obtained from Teijin, Japan. Dopamine hydrochloride (99%) was from Aladdin Chemistry, which the diameter of the yarn (fibril bundles) is 12 μm and the fibrils are elements that pack into yarn which is no more than 100 nm. EPDM-*g*-MAH was supplied by Cromption Corporation, USA. Tris-hydroxymethyl-aminomethane (Tris) was purchased from Ru Ji Bio-Technology Development, Shanghai, China. Hydrochloride was purchased from Chemical Reagent Factory, Wuhan, China. All of the materials were used as received without further treatments. Deionized water was distilled by a Milli-Q water purification system.

Measurements

Fourier transform infrared (FTIR) spectrometer (Thermo Nicolet Nexus, Thermo Nicolet) was used to obtain absorption spectra of the samples between 4000 to 400 cm^{-1} with a resolution of 2 cm^{-1} at room temperature. D/Max-RB X-ray diffraction (XRD) (Rigaku, Japan) with Cu-K_α radiation ($\lambda = 0.154$ nm) was employed to carry out wide angle X-ray diffraction (WAXD) test of the fibers. A scanning rate of 0.2°/min and diffraction angle from 5° to 70° was taken. Bragg's equation, $\lambda = 2d\sin\theta$ was used to calculate the crystallographic spacing. The degrees of crystallinity were calculated according to the reported literature.[21] Thermogravimetric analysis (TGA) was performed on the PPTA by measuring the change in the weight if sample as temperature increased by using Netzsch, STA 499C. Approximately 1.5 mg of the sample was heated from room temperature to 800°C at a heating rate of 10°C/min with nitrogen flow rate of 0.05 L/min. Transmission electron microscopy (TEM) images of PPTA were obtained with a Joel JEM-2001F electron microscope. The samples were first dispersed in ethanol, then a few drops of the dispersion were dripped on a copper grid and evaporated prior to TEM observation, which the sample is separated into fibrils. The surface of PPTA and fracture surface of EPDM-*g*-MAH/PPTA were observed with a scanning electron microscope. All the fractured surfaces were coated with gold–palladium film. The center of the fractured surface of each sample was examined by Toshiba S-4800 scanning electron microscope (SEM, Toshiba, Japan). X-ray photoelectron spectroscopy (XPS) measurements were carried out using a Kratos XSAM-800 spectrometer with an Mg K_α (1253.6 eV) radiator. The X-ray source was run at a reduced power of 200 W. The core-level signals were obtained at a photoelectron takeoff angle of 45° with respect to the sample surface and analyzed by deconvolution of the spectra using the software XPS peak. Tensile strength test was performed according to GB1040-2002 standard. The tensile tests were conducted at a cross head speed of 40 mm/min. The relative conductivity, dielectric constant (ε_r), and dielectric loss (tan δ) were measured as a function of frequency using a HIOKI3532-50 LCR (Japan) impedance analyzer at room temperature. The nuclear magnetic resonance (NMR) cross-polarization magic angle spinning (CPMAS) ^{13}C experiments, with a recycle delay time of 5 s and 2000 scans, were performed on a Bruker Avance III 500 MHz spectrometer at a spinning speed of 10 kHz.

Surface Modification of PPTA

PPTA functionalized with PDOPA nanoshell were produced according to the reported mechanism.[19] The feasible assembly line with some detachable equipment was efficient to continuous functional PPTA (Supporting Information Scheme S1). PPTA@PDOPA with different thickness were made under the same circumstance except dipping–drying cycles through dipping rollers and oxygen drying. Certain concentration of formula solution (2 g L^{-1}) was held by regular dissolving DOPA in a certain amount of Tris–HCl solution of pH 8.5. Pristine dried PPTA fibril was dragged through the vessels containing 2 g L^{-1} DOPA solution. After passing the dipping vessel, oxygen pipe worked to drying, warmed the fibril, and formed nanoshell on the fibril surface through O_2-induced self-polymerization of DOPA monomer. Going in the next dipping vessel, the PPTA was thickened again by stepwise deposit in the presence of trace amount of DOPA, and finally PPTA was *in situ* encapsulated with PDOPA. For match dipping and drying, in general, the dip time and drying time were also set as 2 min. In this case, the dipping–drying step was carried out for 6–10 times. Two sorts of PDOPA modified PPTA with different shell thickness were prepared by regulating the dipping-drying times respectively (denoted PPTA@PDOPAI and PPTA@PDOPAII). Finally, the as-resulted PPTA fiber was washed by distilled water and further dried for storage.

Preparation of EPDM-*g*-MAH/PPTA Composite

The polymer composite materials were prepared by melt blending and hot-press molding. First, a certain amount of EPDM-*g*-MAH was preheated at 180°C, 40 rpm in an internal mixer for 5 min to decrease the viscosity and enable a better wetting of PPTA. Then PPTA, PPTA@PDOPAI and PPTA@PDOPAII which were cut in 5–10 mm in length were respectively incorporated into the rubber matrix in the internal mixer and all of the mixtures were milled at 40 rpm. Sufficient time was necessary to make sure the fiber was well dispersed in the matrix. Finally, all of the specimens were compressed in a mold at 180°C and named EPDM-*g*-MAH/PPTA, EPDM-*g*-MAH/PPTA@PDOPAI and EPDM-*g*-MAH/PPTA@PDOPAII respectively. Three types of rubber composites with different PPTA contents were obtained. The contents of unmodified PPTA and modified PPTA in EPDM-*g*-MAH were 0.1, 0.2, and 0.5 wt %, respectively.

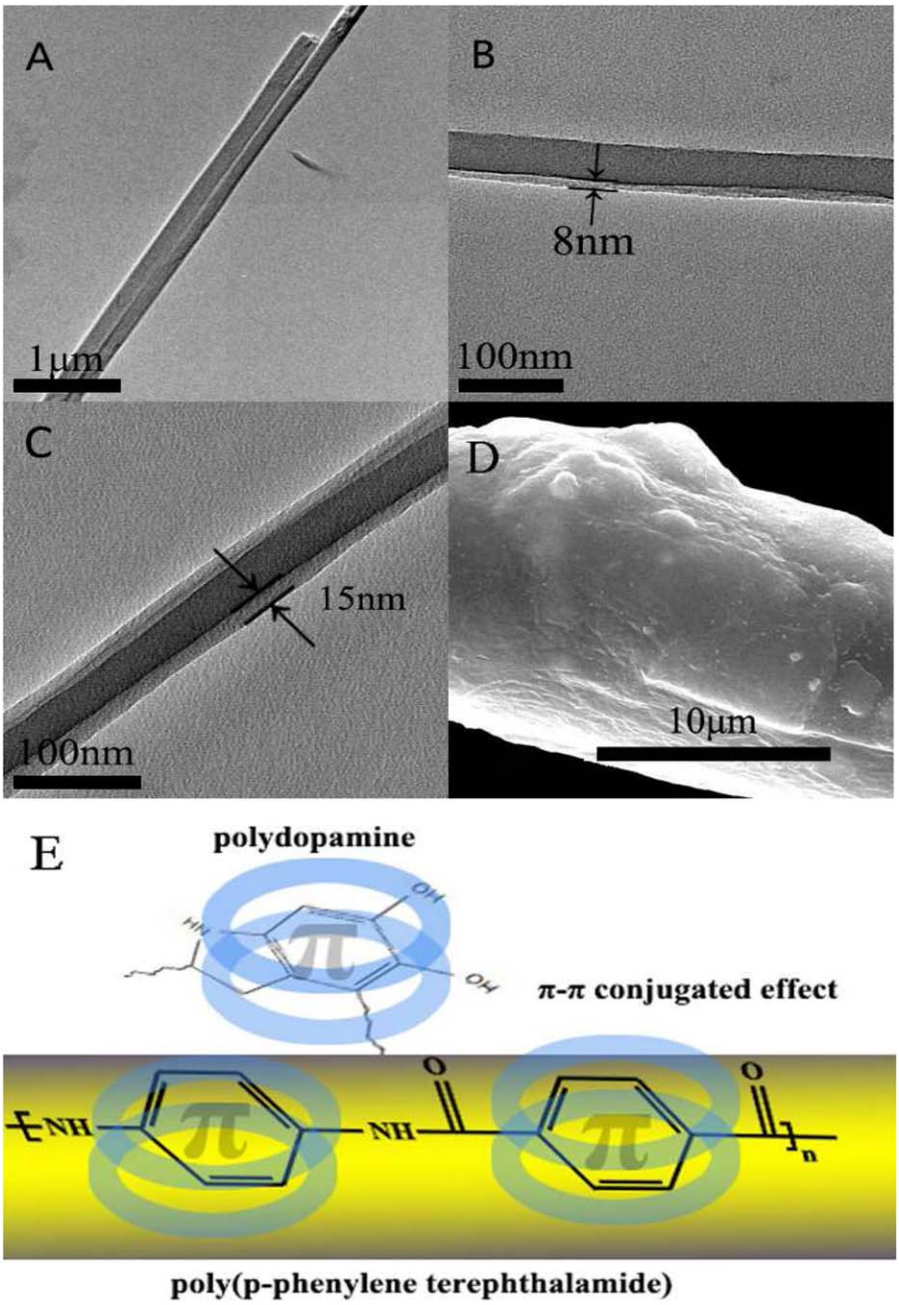

Figure 1. TEM images of PPTA (A), PPTA@PDOPAI (B), PPTA@PDOPAII (C), SEM image of PPTA@PDOPA (D), and schematic diagram of the π–π conjugated effect between PDOPA and PPTA (E). [Color figure can be viewed in the online issue, which is available at wileyonlinelibrary.com.]

RESULTS AND DISCUSSION

In the TEM images of the pristine PPTA [Figure 1(A)], it is clearly shown the unmodified PPTA surface is very smooth as usual without any rough bump. After dipping–drying cycles in DOPA–Tris solution, PDOPA nanoshell had encapsulated on the fiber surface and does not damage the pristine fibril [Figure 1(B,C)]. As the dipping–drying cycles are six times, the thinner one, PPTA@PDOPAI, has a coating layer about 8 nm [Figure 1(B)]. Increasing the dipping–drying cycles to 10 times, the thicker one, PPTA@PDOPAII has an adhesive layer of about 15 nm [Figure 1(C)]. At the first dipping–drying cycle, PPTA soaked by formulate DOPA–Tris solution is hard to be bound totally by DOPA droplets owing to surface tension. After a tough layer around smooth fiber, the PDOPA layer is easier to form and can be controlled by impregnating cycling times.

To demonstrate the morphology of the coated fibril, we further performed SEM observation for PPTA surface morphology. Compared with the pristine PPTA (in Supporting Information Figure S1), the PPTA@PDOPA surface [Figure 1(D)] was grown a rough layer. Smooth PPTA surface has been substituted for rougher organic layer. The growth process is most likely that phenyl ring in PPTA can be strongly associated with DOPA

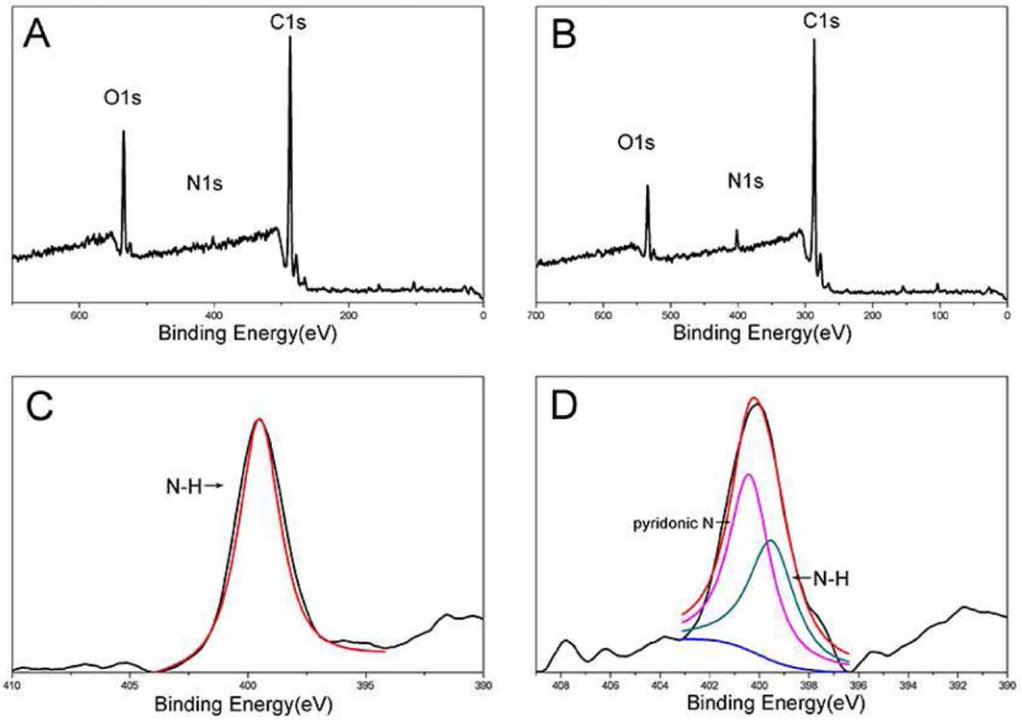

Figure 2. XPS wide-scan spectra and N 1s spectra of pristine PPTA (A,C) and PPTA@PDOPA (B,D). [Color figure can be viewed in the online issue, which is available at wileyonlinelibrary.com.]

molecular due to π–π conjugation interaction [scheme in Figure 1(E)]. Consequently, DOPA was induced to crosslink owing to oxidative self-polymerization of DOPA in certain surroundings. Therefore, PDOPA firmly wrapped around the pristine fibril. Therefore, the functionalized PPTA was modified with active surface; more importantly, the rough layer held its personal property without any surface damage.

The crystal morphologies of PPTA, PPTA@PDOPAI and PPTA@PDOPAII were characterized by XRD. From Supporting Information Figure S2, it can be shown that modified PPTA@PDOPA has the same diffraction peaks as the pristine one, which indicated that the active functionalization strategy offers an approach towards scatheless modification of inert fibril. The degree of crystallinity of PPTA, PPTA@PDOPAI and PPTA@PDOPAII are 64.7, 65.3, and 66.0% respectively, which confirms that the modification did not damage the fibers' crystal morphologies.

FTIR spectra of PPTA, PDOPA and PPTA@PDOPA are shown in Supporting Information Figure S3. Compared to the PPTA@PDOPA, the pristine PPTA exhibits strong bands at 3332 and 1541 cm^{-1}, which can be attributed to the stretching vibrations of —NH— and C═O, respectively. These bands disappear after modification. The appearance of bands at 1251 and 1288 cm^{-1} in the spectrum of PPTA@PDOPA could be assigned to the absorption peaks of the phenolic hydroxyl group (—OH). Additionally, the band at 3406 cm^{-1} can be attributed to the absorption peaks of —NH on indole heterocyclic which implies the presence of PDOPA on the PPTA surface.[20]

The chemical composition of the PPTA surface was determined by XPS. Figure 2 shows the XPS wide-scan and N 1s core-level spectra of the pristine PPTA [Figure 2(A,C)] and the PPTA@PDOPA surface [Figure 2(B,D)]. Both the wide-scan spectra of the pristine PPTA and PPTA@PDOPA surface contain C 1s, N 1s, and O 1s peaks. Nevertheless, the intensity of the N 1s peak in Figure 2(B) is higher than that in Figure 2(A), which indicates that the PDOPA deposited on the surface of PPTA has a higher nitrogen ratio than the pristine PPTA. As shown in Figure 2(C), the N 1s spectrum of the PPTA surface contains only one peak component, which is attributed to the amine (—N—H) species, at a binding energy of 399.5 eV, brought by the *p*-phenylenediamine monomer for synthesizing PPTA. The N 1s core-level spectrum of PPTA@PDOPA showed in Figure 2(D) can be curve-fitted with two peak components, one for the amine (—N—H) species at a binding energy of 399.5 eV and the other for the pyridonic N at a binding energy of 400.4 eV. The —N—H species are attributed to the amine group of PPTA and DOPA, while the pyridonic N is formed by the indole group through structure evolution during the DOPA oxidative self-polymerization.

TGA was used to characterize the thermal stability of PPTA and PPTA@PDOPA (in Supporting Information Figure S4). An interesting phenomenon is that PPTA@PDOPA keeps good thermal stability. From TGA curve, it clearly shows a little weight loss before 100°C and its maximum thermal stability up to 530°C. The result is consistent with the reported literature.[22] Before 100°C, the weight losses mainly resulted in hygroscopic capacity of amido bond in PPTA main chains. Notably, the modified PPTA@PDOPA decreases the hygroscopic capacity loss owing to the newborn hydrophobic PDOPA coating layer. Based on the curves, we can observe that the percentages of weight

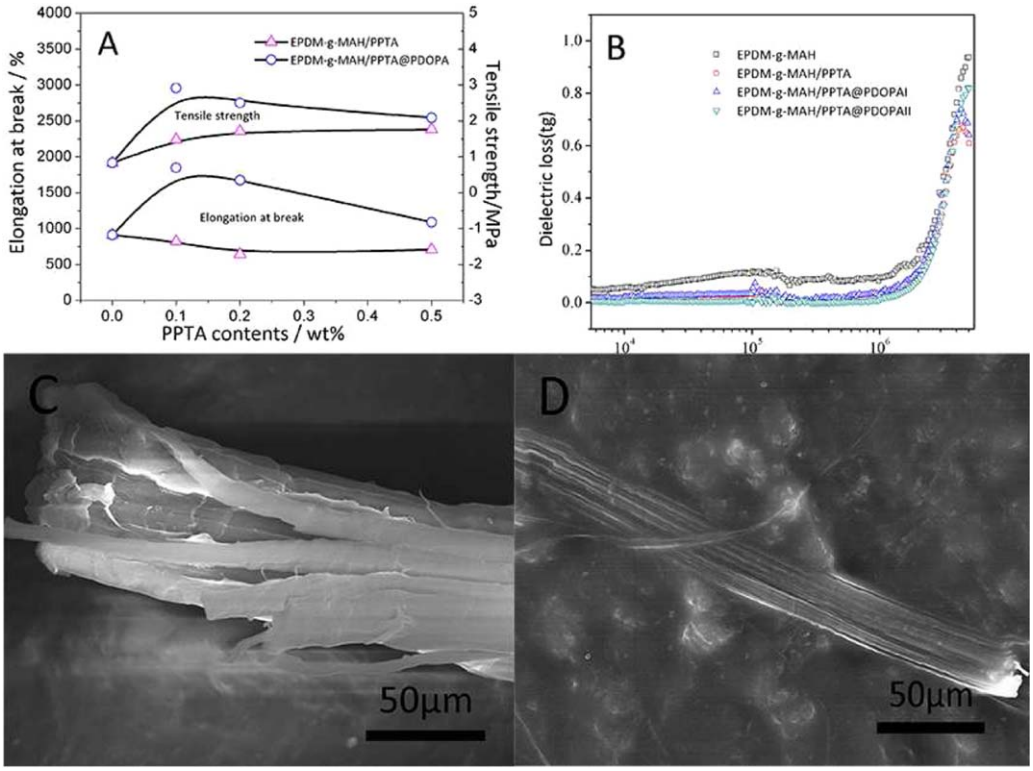

Figure 3. (A) Mechanical properties of EPDM-*g*-MAH/PPTA and EPDM-*g*-MAH/PPTA@PDOPA, (B) dielectric losses of EPDM-*g*-MAH/PPTA and EPDM-*g*-MAH/PPTA@PDOPA, SEM of the unmodified PPTA (C), and modified PPTA (D) mixed in the EPDM-*g*-MAH. [Color figure can be viewed in the online issue, which is available at wileyonlinelibrary.com.]

loss of pure PPTA, PPTA@PDOPAI, and PPTA@PDOPAII are 48.6, 49.6, and 50.4%, respectively. The result shows PPTA@PDOPA holds similar good thermal stability owing to PDOPA nanolayer around PPTA skeleton. It also indicates that the crosslinked PDOPA layer makes more stability than that of pristine PPTA fiber. The main reason could be attributed to the thin nanolayer grown firmly around fibril through π–π conjugation effect.

To further explain the chemical mechanism of the PDOPA reacting with the PPTA on the fibers' surface, solid state NMR was used. As we can see from Supporting Information Figure S5, the resonances on PPTA's spectrum from $\delta = 106.2$–129.9 ppm are identified with the carbon of the benzene ring, and the resonance at $\delta = 155.2$ is assigned to carbonyl.[23] After modification, the resonances of PDOPA at $\delta = 58.0$, 174.1 which can be attributed to cyclized aliphatic carbon and oxygen-bound carbons respectively according to the literature.[20] There is no other new resonances appeared which can confirm that there is no new chemical bond after the modification.

For clarify the active interaction, PPTA and PPTA@PDOPA was used to integrate into EPDM-*g*-MAH matrix through chemical bonding between amino, hydroxyl group, and maleic anhydride functional parts. Their mechanical properties were clearly shown in Figure 3(A). In comparison with EPDM-*g*-MAH/PPTA, EPDM-*g*-MAH/PPTA@PDOPA composite exhibits higher tensile strength and better elongation at break than that of the former. As all typical fiber enhanced composites, the increased tensile strength of EPDM-*g*-MAH/PPTA composite is always accompanied by decreased elongation at break, no matter what fiber content is. Most importantly, for EPDM-*g*-MAH/PPTA@PDOPA composite, the tensile strength and elongation at break simultaneous increase as the modified PPTA content increases from 0 to 0.1 phr, and the maximum values are 2.9 MPa and 1900% as the modified PPTA content reaches 0.1 phr. It is seldom reported in fiber-based polymer composites in which only 0.1 phr PPTA@PDOPA fiber addition enhances sharply the tensile strength and elongation at break of the composite. It is well known that good interface interaction is the main mechanism to explain the increased reinforcement and toughness.[24] In this case, through functional groups interaction, EPDM-*g*-MAH is able to chemically bond with the PDOPA nanolayer, and consequently, PDOPA nanolayer firmly warped PPTA via π–π conjugation effect. When rubber matrix is stretched to a limit for rubber molecular chain, the PDOPA nanolayer will share the stress and transmit to rigid PPTA skeleton. By the aid of the outstanding interfacial adhesion, PPTA@PDOPA integrates into EPDM-*g*-MAH matrix to form a flawless structure. Therefore, the lower content of fibre attributes to enhancing simultaneous tensile strength and elongation at break of composites.

Owing to the same reason, the dielectric losses of composites have also been influenced by their interface adhesion. In comparison with EPDM-*g*-MAH, EPDM-*g*-MAH/PPTA@PDOPA composites can be obviously seen that PPTA@PDOPA decreased the dielectric loss which is similar with that of EPDM-*g*-MAH/

PPTA. It is the main reason that the rigid fiber pushes the segment movement of EPDM polymer chains, and PDOPA nanolayer keeps the PPTA good field-responsive ability [Figure 3(B)]

Figure 3(C,D) show SEM images of EPDM-*g*-MAH/PPTA and EPDM-*g*-MAH/PPTA@PDOPA composites which are fractured in liquid nitrogen. The pristine PPTA fiber slipped out during the strong fracturing impact owing to weak interface adhesion [Figure 3(C)]. And in Figure 3(D), we can seen that the modified PPTA fiber, which is consist of dozens of yarn, was embedded in the matrix although the specimen have also been fractured. It can be proven that modified PPTA could be well compounded with EPDM-*g*-MAH and firmly integrated with the EPDM-*g*-MAH matrix due to the firm interface adhesion. Based on the strategy, it has been developed for homogeneous composites without definite phase separation.

CONCLUSIONS

In summary, we present a simple and efficient strategy to modify PPTA surface with PDOPA. The thickness of the organic layer coating on the surface of PPTA can be controlled by regulating the dipping–drying cycles of the impregnating. PPTA@PDOPA can be compatible with the polymer matrix due to the crosslinked PDOPA which greatly enhances the tensile property and field-responsive ability of EPDM-*g*-MAH. It develops a general modification method for inert fiber to scale factory production and opens a path to enhance the interface adhesion of heterostructure for polymer composites.

ACKNOWLEDGMENTS

The authors are grateful for the financial support from the National Nature Science Foundation of China (No. 51273157), Program for New Century Excellent Talents in University (NCET-10-0659), Key Program of Natural Science Foundation of Hubei Province of China (2013CFA020).

REFERENCES

1. Dobb, M. G.; Johnson, D. J.; Saville, B. P. *J. Polym. Sci. Polym. Phys.* **1977**, *15*, 2201.
2. Lin, T. K.; Wu, S. J.; Lai, J. G.; Shyu, S. S. *Compos. Sci. Technol.* **2000**, *60*, 1873.
3. Simmens, S. C.; Hearle, J. W. S. *J. Polym. Sci. Polym. Phys.* **1980**, *18*, 871.
4. Park, S. J.; Seo, M. K.; Ma, T. J.; Lee, D. R. *J. Colloid Interface Sci.* **2002**, *252*, 249.
5. Wu, G. M.; Hung, C. H.; You, J. H.; Liu, S. J. *J. Polym. Res.* **2004**, *11*, 31.
6. Gu, H. *Mater. Des.* **2008**, *29*, 1671.
7. Feldman, A.; Gonzalez, M. F.; Marom, G. *Macromol. Mater. Eng.* **2003**, *288*, 861.
8. Kalaprasad, G.; Francis, B.; Thomas, S.; Kumar, C. R.; Pavithran, C.; Groeninckx, G.; Thomas, S. *Polym. Int.* **2004**, *53*, 1624.
9. Zhang, Y. H.; Huang., Y. D.; Liu, L.; Cai, K. L. *Appl. Surf. Sci.* **2008**, *254*, 3153.
10. Abdel-Bary, E. M.; El-Nesr, E. M.; Helaly, F. M. *Polym. Adv. Technol.* **1997**, *8*, 140.
11. Liu, L.; Huang, Y. D.; Zhang, Z. Q.; Jiang, B.; Nie, J. *J. Appl. Polym. Sci.* **2001**, *81*, 2764.
12. Wang, J.; Chen, P.; Liu, W.; Li, H.; Jia, C.; Lu, C.; Wang, B. *J. Appl. Polym. Sci.* **2011**, *121*, 2804.
13. Jia, C.; Chen, P.; Liu, W.; Li, B.; Wang, Q. *Appl. Surf. Sci.* **2011**, *257*, 4165.
14. Su, M.; Gu, A.; Liang, G.; Yuan, L. *Appl. Surf. Sci.* **2011**, *257*, 3158.
15. Tamargo-Martínez, K.; Martínez-Alonso, A.; Gracia, M.; Paredes, J. I.; Tascón, J. M. D.; Montes-Morán, M. A. *Compos. A: Appl. Sci. Manuf.* **2013**, *50*, 102.
16. Thakur, V. K.; Yan, J.; Lin, M. F.; Zhi, C.; Golberg, D.; Bando, Y.; Sim, R.; Lee, P. S. *Polym. Chem.* **2012**, *3*, 962.
17. Xu, C.; Xu, K.; Gu, H.; Zheng, R.; Liu, H.; Zhang, X.; Guo, Z.; Xu, B. *J Am. Chem. Soc.* **2004**, *126*, 9938.
18. Thakur, V. K.; Lin, M. F.; Tan, E. J.; Lee, P. S. *J. Mater. Chem.* **2012**, *22*, 5951.
19. Lee, H.; Dellatore, S. M.; Miller, W. M.; Messersmith, P. B. *Science* **2007**, *318*, 426.
20. Dreyer, D. R.; Miller, D. J.; Freeman, B. D.; Paul, D. R.; Bielawski, C. W. *Langmuir* **2012**, *28*, 6428.
21. Castro-Muñiz, A.; Martínez-Alonso, A.; Tascón, J. M. D. *Carbon* **2008**, *46*, 985.
22. Perepelkin, K. E.; Andreeva, I. V.; Pakshver, E. A.; Morgoeva, I. Y. *Fibre Chem.* **2003**, *35*, 265.
23. English, A. D. *J. Polym. Sci. Polym. Phys.* **1986**, *24*, 805.
24. Tavakoli, M.; Katbab, A. A.; Nazockdast, H. *J. Appl. Polym. Sci.* **2012**, *123*, 1853.